3D MoS_2-Graphene Composite as Catalyst for Enhanced Efficient Hydrogen Evolution

K.M. SARODE[a], U. D. PATIL[a], D. R. PATIL[a*]

[a]Asistant professor R.C. Patel Arts,Commerce &Science College, Shirpur, 425405, Maharashtra, India

[a*]Principal, R.C. Patel Arts,Commerce &Science College, Shirpur, 425405, Maharashtra, India

***Corresponding Author E-mail:** dr.drpatil@gmail.com

Abstract

In this work, Three-dimensional (3D) molybdenum disulfide/graphene (MoS_2-RGO) composites were synthesized by hydrolysis of lithiated MoS_2 ($LiMoS_2$). These MoS_2-RGO composites exhibit sheets-like morphology, and show promising results of electrocatalytic activities in hydrogen evolution reaction (HER) than MoS_2, with a low over potential of approximately 186 mV, a small Tafel slope of 66 mV/dec , as well as excellent long-term durability. The superior electrochemical performance should be attributed to the synergic effects between the MoS_2 and RGO.

Keywords: MoS2, MoS2-graphene composites, Hydrogen evolution reaction, Synergic effect**.**

Introduction

Today, fossil fuels are known as the main energy sources with their disadvantages such as global warming, limited resources, and the environmental pollution. Various efforts are being considered to use other energy sources instead of fossil fuels to overcome these disadvantages. Currently, Water splitting through photo electrochemical or electrochemical method has recently been regarded as one of the most promising hydrogen production technologies because of its pollution-free, recyclability and economical way [1-4]. The major challenge of water electrolysis is to development of high-performance and cost- effective electrocatalysts for the hydrogen evolution reaction (HER). Up to date, noble metal, such as platinum-based electrocatalysts have been known as efficient catalysts for hydrogen generation [5-6]. However, their widespread application has been restricted by their high cost and low-earth abundance. In this circumstance, it is therefore necessary to synthesize material suitable for electrochemical studies as an alternative to platinum.

In recent years, noble-metal-free electrocatalysts include transition metal chalcogenides (MX_2, Where M = Mo or W and X = S or Se) have shown enormous potential for the HER [7-9]. Among these catalysts, molybdenum disulfide (MoS_2)-based electrocatalysts for HERs have been developed as promising alternatives for platinum due to their high activity and low cost[10,11]. However, poor electrical conductivity and insufficient numbers of active sites of MoS_2 have limited the overall electrocatalytic performance [12 13]. To circumvent these problems, designing MoS_2-based materials with more active edge sites and good conductivity would be an effective way to improve

the electrocatalytic HER. MoS_2 has been hybridized with conductive materials such as carbon nanotubes [14], conductive polymer [15] and graphene [16 19]. Compared to other conductive material, graphene has larger specific surface area and excellent electronic conductivity and stability [20, 21]. Based on these features, the combination of MoS_2 and graphene should be a good solution to overcome the above problem.

Herein, we have synthesized MoS_2-RGO composites for Excellent HER activity using hydrolysis of lithiated MoS_2 ($LiMoS_2$) method. The composites structure was examined using Field Emission scanning electron microscopy (FESEM), X ray diffraction (XRD) patterns, high-resolution transmission electron microscopy (HR-TEM) and X-ray photoelectron spectroscopy (XPS). The obtained composite exhibited high HER activity and stability simultaneously.

Experimental

Synthesis of MoS2-RGO composites

The RGO was prepared through an improved Hummer's method followed by chemical reduction in hydrazine hydrate, as described in more detail in previous publication [22 23]. In brief, 1.0 g bulk MoS2 powder was added to 10 mL 1.6M n-butyllithium solution in hexane in a flask filled with N2 gas [24], the mixture was soaked at room temperature for 48 h. Afterwards, the produced LixMoS2 was filtered and washed repeatedly with hexane to remove excessive lithium and then dried under the nitrogen atmosphere. Next, 100 mg of LixMoS2 was added into 20 ml deionized water and ultrasonicated for 1 h to obtained aqueous suspension of MoS2 nanosheets. The reactions are described as follows: [25]

$$MoS_2 + n\text{-}BuLi \longrightarrow LiMoS_2 + 1/2C_8H_{18} \quad (1)$$

$$LiMoS_2 + H_2O \longrightarrow (MoS_2)_{\text{exfoliated layers}} + LiOH + 1/2H_2 \quad (2)$$

Then, the synthesized RGO nanosheets were dispersed in ethanol (3 mg/mL) and ultrasonicated for 30 min to produce RGO suspension. The produced RGO suspension was then slowly added to the MoS2 layers and sonicated for 2 h at 10^{O}C, the resultant composite materials suspension was stirred at room temperature for 3 days and heated in oil bath at 80°C under a water cooled condenser for 24 h. The resultant precipitate was collected by centrifugation at 8000 rpm for 15 min, washed several times with deionized water, ethanol and lastly dried in vacuum oven at 80^{O}C overnight. The different mass ratios of LiMoS2/RGO are taken as 100/12.5, 100/25, 100/50 and 100/100, named as MoS2-RGO-1, MoS2-RGO-2, MoS2-RGO-3 and MoS2-RGO-4. As a control, the restacked MoS2 (MoS2) was also prepared without adding any RGO. The Synthesis procedure for MoS2-RGO composites is illustrated in Scheme 1.

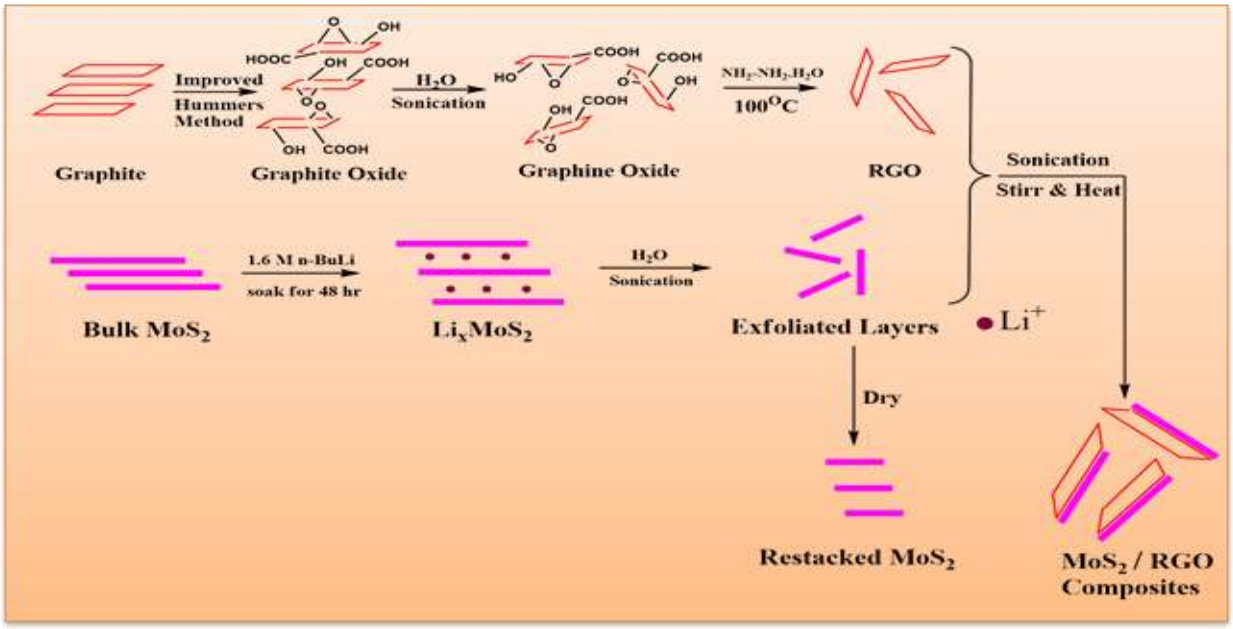

Scheme 1: The synthetic route of the MoS2-RGO composites.

Material characterizations

The morphology and structure of the samples were characterized by field-emission scanning electron microscopy (FESEM, M o d e l Zeiss/Ultra 55), high-resolution transmission electron microscopy (HRTEM, TecnaiG2, F30), X-ray diffraction (XRD, EMPYREAN diffractometer employing a Cu-Ka source), X-ray photoelectron spectroscopy (XPS, AXIS ULTRA).

Electrochemical measurements

Electrochemical measurements were carried out with a computer controlled potentiostat electrochemical workstation (CHI660D) in a standard three-electrode system with a disk glassy carbon electrode (GCE, 3 mm in diameter) as the working electrode. Pt wire and saturated calomel electrode (SCE) were used as counter and reference electrode, respectively. Typically, 5 mg of sample and 50 μL Nafion solution (5 wt %) were dispersed in 0.5 mL water-ethanol mixture solution by sonicating for 30 min to form a homogeneous ink. Then 5 μL of the dispersion solution was loaded onto a disk glassy carbon electrode. Electrolyte was degassed by bubbling N2 for 20 min prior to each experiment. Linear sweep voltammetry with scan rate of 10 mV s^{-1} was conducted in 0.50 M H2SO4 solution from 0.1 to -0.5 V vs RHE. The electrochemical impedance spectroscopy (EIS) measurements were carried out in the same configuration at an overpotential η= 200 mV from 105 to 0.1 Hz with an AC voltage of 10 mV.

Results and Discussion

The as-synthesized samples with different mass percentages of RGO in the composites are 0% 12%, 25% 50% and 100% for labelled as MoS2, MoS2-RGO-1, MoS2-RGO-2, MoS2-RGO-3 and MoS2- RGO-4, respectively. Their morphologies recorded by FESEM are shown in Fig. 1. As shown in Fig. 1a, the bulk MoS2 exhibits tightly stacked layered structures with largely micrometer-sized

inerratic sheets. After exfoliation, the morphology of restacked MoS_2 interestingly changed to highly scattered nanoflake in Fig. 1b. It is also noted that the size and thickness of the nanosheets were significantly decreased relative to the bulk MoS_2. Pure RGO exhibits corrugated and curled nanosheet structure (Figure 1c). As shown in Fig. 1(d)–(f), the MoS_2-RGO composites with different contents of RGO exhibits a sheets-like morphology with a diameter from submicrometers to nearly one micrometers, which was formed during the hydrolysis of lithiated MoS_2 ($LiMoS_2$) process. Such 3D network structure would be beneficial for shortening the electron diffusion channel due to the highly electroactive area [26], leading to superior HER performance. Moreover, the 3D network structure would compensate the volume change [26] during the long time test in acid media. However, the 3D network structure becomes less obvious when the RGO volume is added to 100% (Figure 1f).The excess amount of RGO might decrease the amount of active sites and block the charge transfer from electrolyte to MoS_2, leading to inferior HER activity [27].

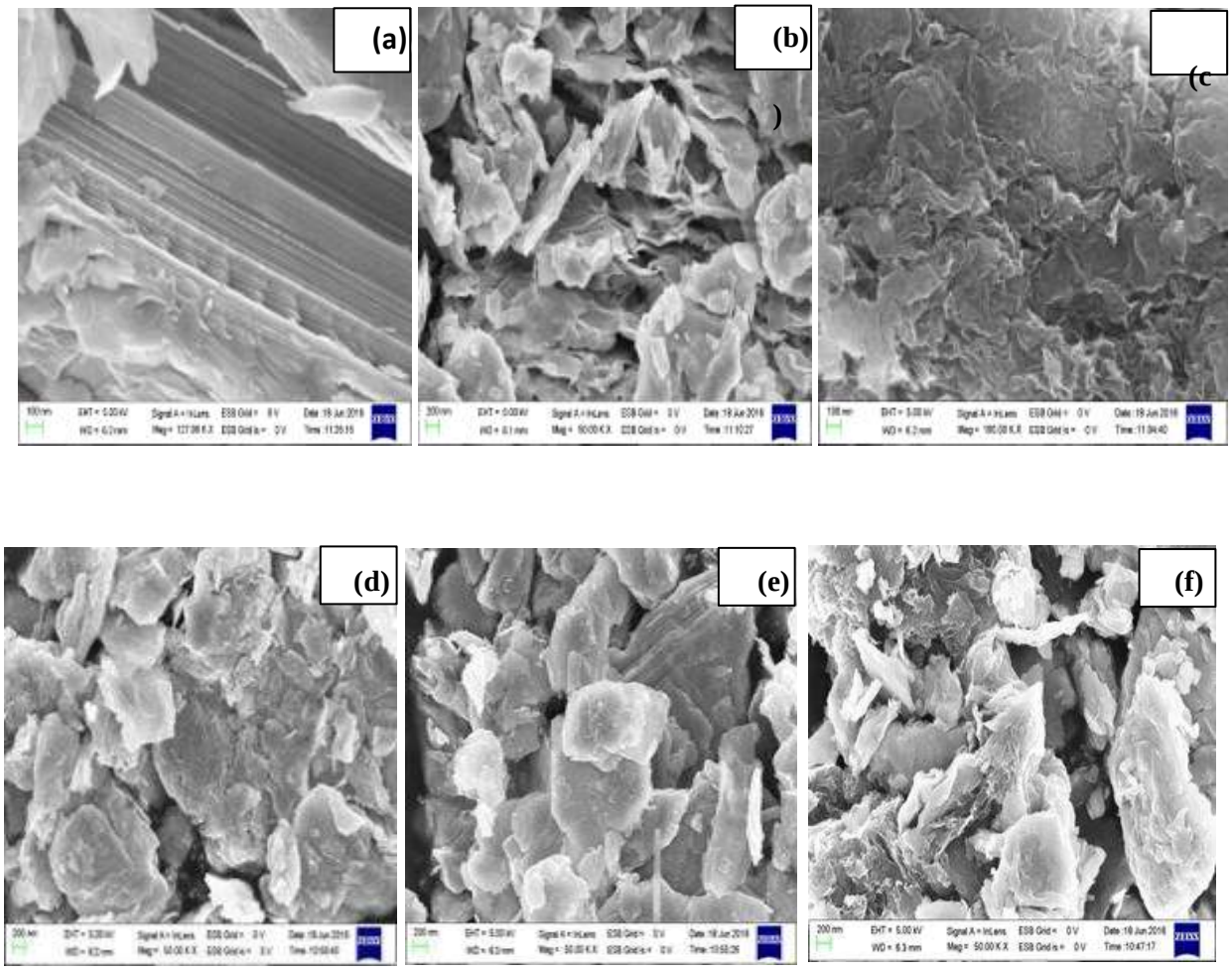

Fig. 1: FESEM images of (a) bulk MoS_2, (b) MoS_2, (c) RGO, (e) bulk MoS_2, (f) MoS_2-RGO-2, (g) MoS_2-RGO-3, (h) MoS_2-RGO-4.

The XRD patterns of the as–prepared bulk MoS_2, MoS_2, RGO, MoS_2-RGO-1, MoS_2-RGO-2, MoS_2-RGO-3 and MoS_2-RGO-4 were described in previous publication [28] and Figure 2. The bulk

MoS_2 had hexagonal structure (JCPDS card No. 37–1492), the strong peak at 2θ ≅ 14.5 with a d-spacing of 0.64 nm signifies a well-stacked layered structure along the c axis. After lithiation exfoliation without RGO, restacked MoS_2 shows lower peak intensity, indicating the decrease of crystallinity. For MoS_2-RGO composites, essentially retains the position of the diffraction peaks of MoS_2, while the intensity of peak continuously decreases with increasing percentages of RGO in the composites. We can also detect the (002) diffraction peak of graphene at 2θ ≅ 24, indicating that the RGO nanosheets seldom stack together.

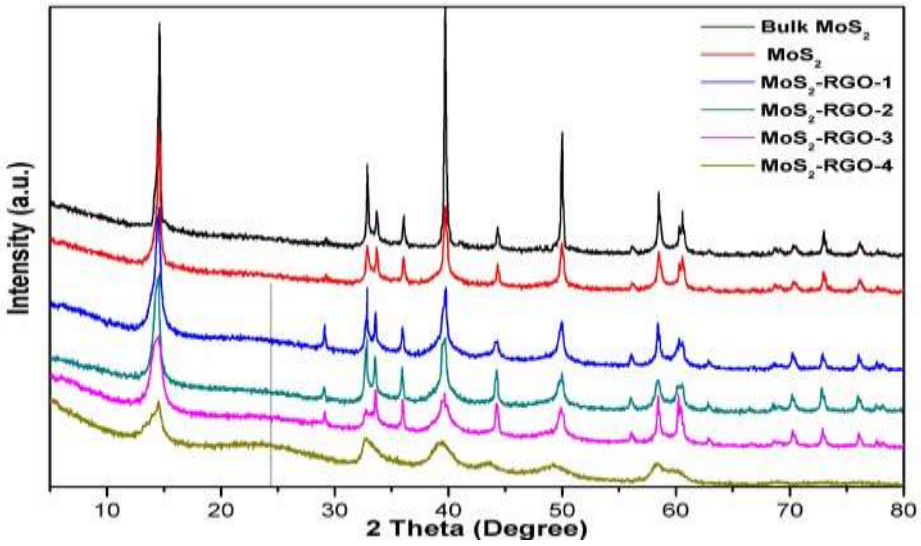

Fig. 2: XRD patterns of bulk MoS2, MoS2, MoS2-RGO-1, MoS2-RGO-2, MoS2-RGO-3 and MoS2- RGO-4samples.

The microstructure of the MoS2-RGO composite (MoS2-RGO-3) was characterized by HRTEM, as shown in Fig. 3. It can be observed that MoS2 nanosheets consist of few layers with an interlayer of 0.61 nm, which are supported on the surface of graphene. Notice that the crystal fringes are discontinuous, indicating the existence of defects [29]. Such defects might provide more active sites, which makes MoS2-RGO-3 composite appropriate as advanced catalysts for HER.

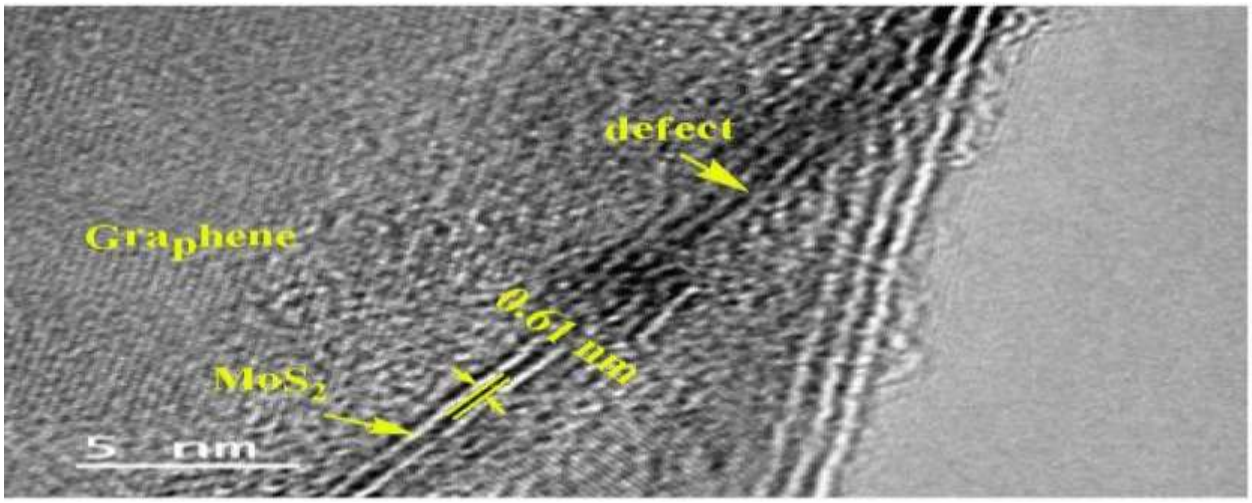

Fig. 3: HRTEM images of MoS2-RGO-3Sample**.**

X-ray photoelectron spectroscopic (XPS) measurements were carried out to further investigate the chemical composition of MoS_2-RGO-3. As shown in the survey spectrum in Fig. 4A, the elements of Mo, S, C and O can be clearly identified with the Mo/S atomic ratio of ~1:2, in good agreement with the stoichiometric value in MoS_2. Fig. 4B depicts Mo 3d and S 2s XPS spectra of MoS_2-RGO-3, where the characteristic peaks located at 229.6 and 232.6 eV are ascribed to Mo $3d_{5/2}$ and $3d_{3/2}$ of tetravalence molybdenum ion (Mo^{4+}), respectively, otherwise, the peak at 226.8 eV corresponds to S 2s of MoS_2. For S 2p region, which is shown in Fig. 3d, the peaks at 162.3 and 163.3 eV can be assigned, respectively, to the S $2p_{3/2}$ and $2p_{1/2}$ orbitals of divalent sulfide ions (S^{2-}). The C1s XPS spectrum of MoS_2-RGO-3 as shown in Fig. 4c, there are three functional groups associated with C- C at 284.8 eV, C-O at 286.85 eV and C= O at 287.5 eV. In contrast with initial GO, the peaks of all oxygen containing functional groups are decreased, it confirms that a reduction process of GO has occurred.

XI-

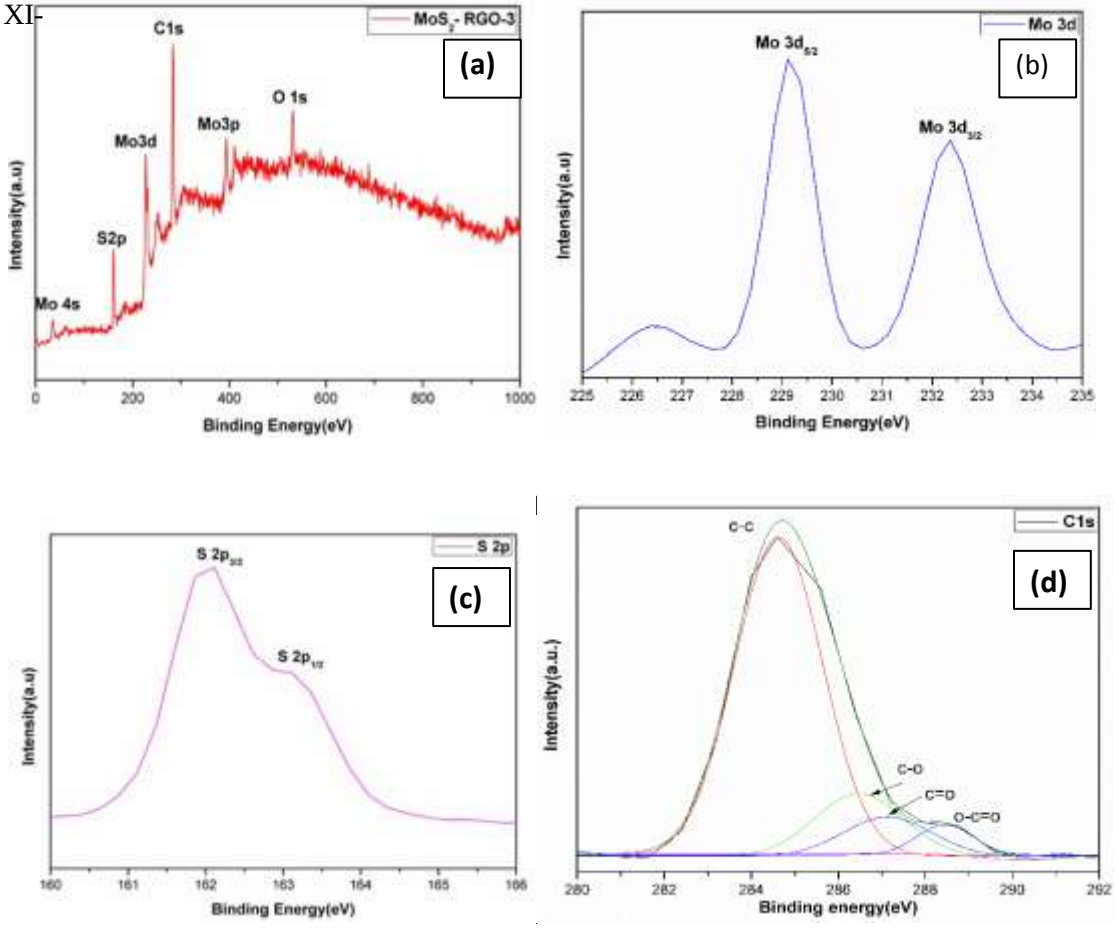

Fig. 4: X-ray photoelectron spectra of (A) Survey, (B) Mo 3d (C) S 2p, (d) C 1s binding energy regions for MoS_2-RGO-3 Sample.

The XPS spectrum of C 1s region (Figure 4d), the peak intensity of C–O at 286.85 eV and C=Oat 287.5 eV species is very weak, In contrast with initial GO, the peaks of all oxygen containing functional groups are decreased that indicates a considerable reduction of GO by hydrothermal reaction.

The electrocatalytic activity of all the samples was investigated in 0.5 M H_2SO_4 solution by linear sweep voltammetry (LSV) using a three–electrode setup. Fig. 5A shows the polarization curves (j-V plot) for MoS_2, MoS_2-RGO-1, MoS_2-RGO-2, MoS_2-RGO-3 and MoS_2-RGO-4 materials at a scan rate of 10 mV s^{-1} with a rotation rate of 2500 rpm. From Fig. 5A, it is clearly seen that the sample (MoS_2) prepared without RGO showed the lowest HER activity in terms of current density and onset potential. However, with increase different mass percentages of RGO in the composites, the MoS_2-RGO-1, MoS_2-RGO-2, MoS_2-RGO-3 and MoS_2-RGO-4 materials show an excellent performance in HER activity. The MoS_2- RGO-3 sample has a small onset overpotential (η=186 mV) compared to other four samples (Table 1), beyond which the cathodic current rises rapidly under more negative potentials, indicating the superior HER activity. The super catalytic performance of MoS_2-RGO-3 was attributed to the 3D architecture with abundance of exposed active sites as analyzed by HRTEM. The MoS_2-RGO-4 composite exhibited low activity because excess amount of RGO might decrease the amount of active sites and block the charge transfer, our result similar to previous reported [27].

Sample	Onset potential (mV)	Tafel slope (mV/dec)
MoS2	198	162
MoS2-RGO-1	216	98
MoS2-RGO-2	189	96
MoS2-RGO-3	186	66
MoS2-RGO-4	270	215

Table 1: Electrochemical analysis of various MoS_2-RGO composite catalysts.

Fig. 5B shows the Tafel plots for the all catalysts. The Tafel slope determined by Tafel plots andthe linear portions are fitted into the Tafel equation, h = a +b log (j0) (a is the Tafel constant b is the Tafel slope , j0is the exchange current density), which reveals the intrinsic properties of the electrocatalyst materials [30,31]. A small Tafel slopes of 66 mV/dec for MoS2-RGO-3, which is much smaller than the Tafel slope of the MoS2 (~162 mV/dec) and other MoS2-RGO samples (MoS2-RGO-1 ~98 mV/dec, MoS2-RGO-2 ~ 96 mV/dec and MoS2-RGO-4 ~ 215 mV/dec). In principle, a lower Tafelslope means that a faster increase of HER rate with the increasing potential [32]. Compared with MoS2,MoS2-RGO-3 shows high exchange current density of 2.53×10^{-5} A/cm^2. The smallest slope of MoS2- RGO-3 is owing to the synergetic effect of the heterogeneous structure provided by MoS2-RGO interface. The structure of interface provides a large number of active catalytic sites, which is beneficial to raise the reaction rate [33].

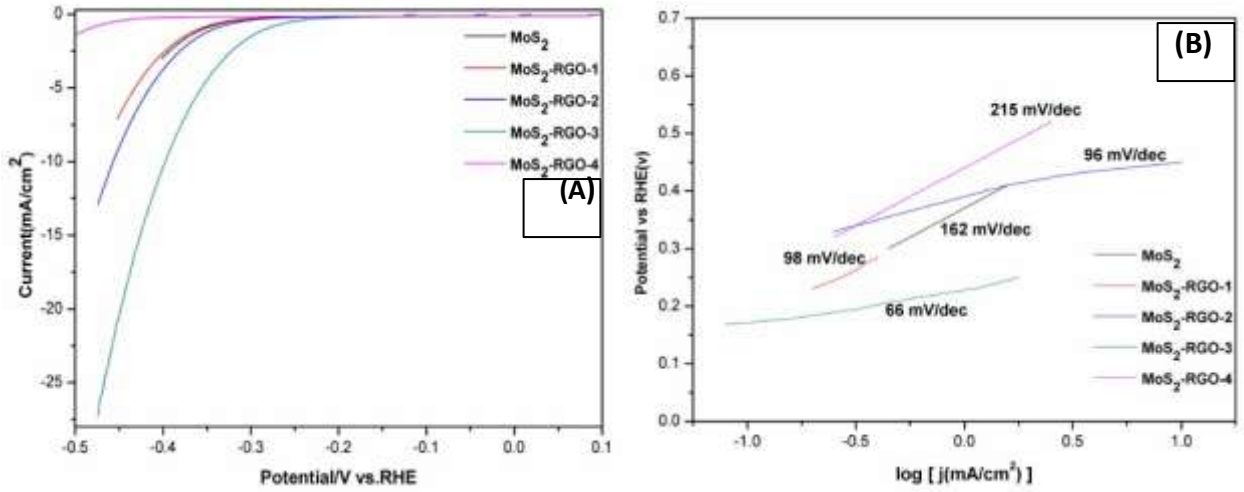

Fig.5 (A) Linear sweep voltammogram curves for five different MoS2-RGO; **(B)** Tafel plots of five different MoS2-RGO;

Electrochemical impedance spectroscopy (EIS) is a powerful technique to characterize interfacial reactions and electron-transfer kinetics in HER. Fig.6A shows the Nyquist plots of the EIS spectra for the all catalysts. MoS_2-RGO-3 composite shows much lower charge transfer resistance than the other four samples, indicating enhanced conductivity of MoS_2-RGO-3. The smaller resistance of MoS_2-RGO-3 means much faster electron transfer and improved efficiency for HER.

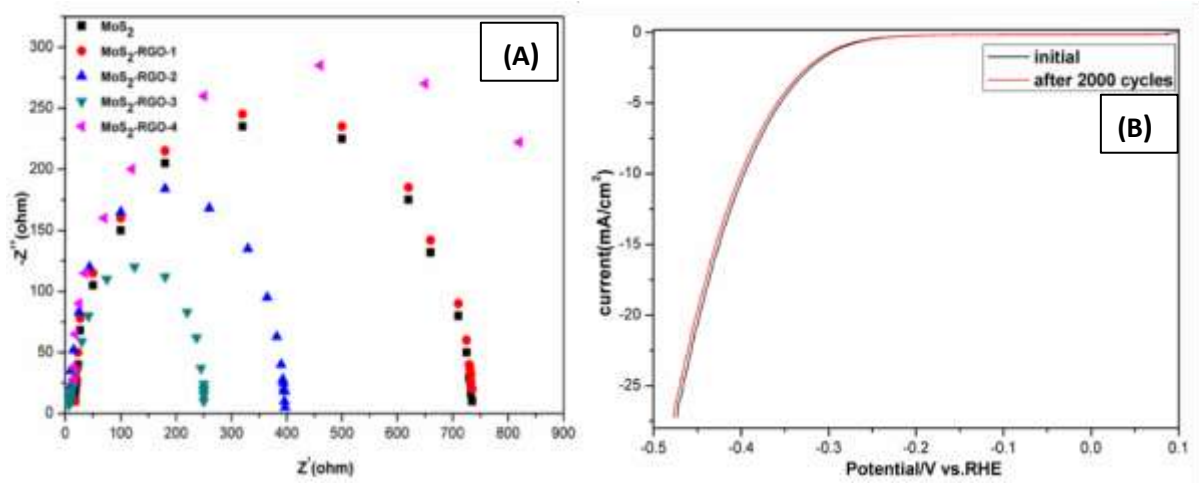

Fig.6 (A) Nyquist plots of EIS for various MoS2-RGO catalysts,(B)Stability test for MoS2-RGO-3 sample in 0.5 M H2SO4 solution at a scan rate of 200 mV/s.

We further investigated the durability of MoS_2-RGO-3 composite. The as-synthesized MoS_2-RGO-3 catalysts show negligible loss even after continuous 2000 cycles and maintain the current density at 97.3% compared with its initial value (Figure 6 B), indicating the superior long-time stability of the MoS_2-RGO-3 composite in acid media. This could be attributed to the 3D network structures [34] and intimate contact [35, 36] between the MoS_2 nanosheets and RGO hydrogel, decreasing the volume change during the long time test in acid media [37].

Conclusion

We have synthesized MoS_2-RGO composites via a hydrolysis of lithiated MoS_2 ($LiMoS_2$) approach. When an appropriate amount of RGO was used, the resulting MoS_2-RGO composite exhibited significantly higher HER activity with lower overpotential of 186 mV, a relatively small Tafel slope of 90 mV/dec and high exchange current density of $2.53 \times 10^{-5} A/cm^2$ than MoS_2. Our durability of MoS_2-RG-3 composite results suggests that as catalyst for many applications in energy and environment fields.

References

[1] L. Ji, J. Wang, L. Guo, Z. Chen, In situ O2-emission assisted synthesis of molybdenum carbide nanomaterials as an efficient electrocatalyst for hydrogen production in both acidic and alkaline media, J. Mater. Chem. A, 5 (2017) 5178-5186.

[2] Y.Y. Chen, Y. Zhang, W.J. Jiang, X. Zhang, Z. Dai, L.J. Wan, J.S. Hu, Pomegranate-like ,P-Doped Mo2C@C Nanospheres as Highly Active Electrocatalysts for Alkaline Hydrogen Evolution, ACS Nano, 10 (2016) 8851-8860.

[3] B. Rausch, M. D. Symes, G. Chisholm, L. Cronin, Decoupled Catalytic Hydrogen Evolution from a Molecular Metal Oxide Redox Mediator in Water Splitting. Science 345 (2014), 1326−1330.

[4] S. Li, Y. Wang, S. Peng, L. Zhang, A.M. Al-Enizi, H. Zhang, X. Sun, G. Zheng, Co-Ni-Based Nanotubes/Nanosheets as Efficient Water Splitting Electrocatalysts, Adv. Energy Mater.,6 (2016) 1501661.

[5] L. Peng, Y. Nie, L. Zhang, R. Xiang, J. Wang, H. Chen, K. Chen, Z. Wei, Self-assemblyand Preshaping-assisted Synthesis of Molybdenum Carbide Supported on Ultrathin Nitrogendoped Graphitic Carbon Lamellas for the Hydrogen Evolution Reaction, ChemCatChem, 9 (2017) 1588-1593.

[6] Z.W. Seh, J. Kibsgaard, C.F. Dickens, I. Chorkendorff, J.K. Nørskov, T.F. Jaramillo, Science 355(2017) eaad 4998.

[7] Gao, M. R.; Lin, Z. Y.; Zhuang, T. T.; Jiang, J.; Xu, Y. F.; Zheng, Y. R.; Yu, S. H. Mixed-solution Synthesis of Sea Urchin-like NiSe Nanofiber Assemblies as Economical Pt-Free Catalysts for Electrochemical H2 Production. J. Mater. Chem. 2012, 22, 13662−13668.

[8] Tang, H.; Dou, K. P.; Kaun, C. C.; Kuang, Q.; Yang, S. H. MoSe2 Nanosheets and Their Graphene Hybrids: Synthesis, Characterization and Hydrogen Evolution Reaction Studies. J. Mater. Chem. A 2014, 2, 360−364.

[9] T. Liu, C. Wang, X. Gu, H. Gong, L. Cheng, X. Shi, L. Feng, B. Sun and Z. Liu, Adv. Mater., 2014, 26, 3433-3440.

[10] Laursen, A. B.; Kegnæs, S.; Dahl, S.; Chorkendorff, I. Molybdenum sulfides—Efficient and viable materials for electro- and photoelectrocatalytic hydrogen evolution. Energy Environ. Sci. 2012, 5, 5577–5591.

[11] Kibsgaard J, Chen Z, Reinecke BN, Jaramillo TF.Engineering the surface structure of MoS2 to preferentially expose active edge sites for electrocatalysis. Nat Mater 2012;11:963e9.

[12] Zhang Y, Zuo L, Zhang L, Huang Y, Lu H, Fan W and Liu T 2016 Cotton wool derived carbon fiber aerogel supported few-layered MoSe2 nanosheets as efficient electrocatalysts

for hydrogen evolution ACS Appl. Mater. Interfaces 8 7077

[13] Laursen, A. B.; Kegnæs, S.; Dahl, S.; Chorkendorff, I. Molybdenum sulfides—Efficient and viable materials for electro- and photoelectrocatalytic hydrogen evolution. Energy Environ. Sci. 2012, 5, 5577–5591.

[14] Shi Y, Wang Y, Wong JI, Tan AYS, Hsu CL, Li LJ, et al. Self- Assembly of hierarchical MoSx/CNT nanocomposites (2<x<3). Sci Rep-uk 2013;3:1e8.

[15] Wang T, Zhuo J, Du K, Chen B, Zhu Z, Shao Y, et al. Electrochemically fabricated polypyrrole and MoSx copolymer films as a highly active hydrogen evolution electrocatalyst. Adv Mater 2014;26:3761e6.

[16] Li Y, Wang H, Xie L, Liang Y, Hong G, Dai H. MoS2 nanoparticles grown on graphene: an advanced catalyst for the hydrogen evolution reaction. J Am Chem Soc 2011;133:7296e9.

[17] Zhou W, Zhou K, Hou D, Liu X, Li G, Sang Y, et al. Threedimensional hierarchical frameworks based on MoS2 nanosheets self-assembled on graphene oxide for efficient electrocatalytic hydrogen evolution. ACS Appl Mater Interfaces 2014;6:21534e40.

[18] Liao L, Zhu J, Bian X, Zhu L, Scanlon MD, Girault HH, et al. MoS2 formed on mesoporous graphene as a highly active catalyst for hydrogen evolution. Adv Funct Mater 2013;23:5326e33.

[19] Chen S, Duan J, Tang Y, Jin B, Qiao S. Molybdenum sulfide clusters-nitrogen-doped graphene hybrid hydrogel film as an efficient three-dimensional hydrogen evolution electrocatalyst. Nano Energy 2015;11:11e8.

[20] Allen MJ, Tung VC, Kaner RB. Honeycomb carbon: a review of graphene. Chem Rev 2009;110:132e45.

[21] Chang K, Chen W. L-cysteine-assisted synthesis of layered MoS2/graphene composites with excellent electrochemical performances for lithium ion batteries. ACS Nano 2011;5:4720e8.

[22] D.C. Marcano, D.V. Kosynkin, J.M. Berlin, A. Sinitskii, Z. Sun, A. Slesarev, L.B. Alemany, W. Lu, J.M. Tour, Improved synthesis of graphene oxide, (2010).

[23] S. Stankovich, D.A. Dikin, R.D. Piner, K.A. Kohlhaas, A. Kleinhammes, Y. Jia, Y. Wu, S.T. Nguyen, R.S. Ruoff, Synthesis of graphene-based nanosheets via chemical reduction of exfoliated graphite oxide, carbon, 45 (2007) 1558-1565.

[24] G. Eda, H. Yamaguchi, D. Voiry, T. Fujita, M. Chen, M. Chhowalla,2011 Nano letters 11, 5111-5116.

[25] G. Du, Z. Guo, S. Wang, R. Zeng, Z. Chen, H. Liu, 2010 Chemical Communications 46, 1106-1108.

[26] K. Chang, W.X. Chen, ACS Nano 6 (2011) 4720.

[27] F.K. Meng, J.T. Li, S.K. Cushing, M.J. Zhi, N.Q. Wu, Journal of American Chemical Society 135 (2013) 10286

[28] Komal M Sarode, Umesh D Patil, Dilip R Pati, International Journal of Current Advanced Research, 07(1), pp. (2018) 9283-9288.

[29] J.X. Xie, H. Zhang, S. Li, R.X. Wang, X. Sun, M. Zhou, J.F. Zhou, X. Wen, D Lou, Y. Xie, Advanced Materials 25 (2013) 5807.

[30] X. Ren, L. Pang, Y. Zhang, X. Ren, H. Fanac, S. Liu, One-step hydrothermalsynthesis of monolayer MoS2quantum dots for highly efficientelectrocatalytic hydrogen evolution, J. Mater. Chem. A 3 (2015) 10693–10697.

[31] S. Xu, D. Li, P. Wu, One-pot facile, and versatile synthesis of monolayer-

MoS2/WS2quantum dots as bioimaging probes and efficient electrocatalystsfor hydrogen evolution reaction, Adv. Funct. Mater. 25 (2015) 1127–1136.

[32] Feng Li, Jing Li, Xiaoqing Lin, Xinzhe Li, Yiyun Fang, Lixin Jiao, Xincai An, Yan Fu, Jun Jin, Rong Li, Designed synthesis of multi-walled carbon nanotubes@Cu@MoS2 hybrid as advanced electrocatalyst for highly efficient hydrogen evolution reaction, Journal of Power Sources 300 (2015) 301-308.

[33] H.L. Li, K. Yu, C. Li, Z. Tang, B.J. Guo, X. Lei, H. Fu, Z.Q. Zhu, Charge-transferinduced high efficient hydrogen evolution of MoS2/grapheme cocatalyst, Sci.Rep. 12 (2015) 1–11.

[34] W.J. Zhou, K. Zhou, D.M. Hou, X.J. Liu, G.Q. Li, Y.H. Sang, H. Liu, L.G. Li, S.W. Chen, ACS Applied materials &interfaces 6 (2014) 21534.

[35] Q.J. Xiang, J.G. Yu, M. Jaroniec, Journal of American Chemical Society 134 (2012) 6578.

[36] A.B. Laursen, S. Kegnaes, S. Dahl, I. Chorkendorff, Energy & Environmental Science 5 (2012) 5577.

[37] K. Chang, W.X. Chen, ACS Nano 6 (2011) 4720.